

Article

The Influence of Blood and Serum Microenvironment on Spin-Labeled Magnetic Nanoparticles

Tomasz Kubiak ^{1,2} 

¹ Faculty of Physics, Adam Mickiewicz University in Poznań, Uniwersytetu Poznańskiego 2, 61-614 Poznań, Poland; kubiakt@amu.edu.pl

² Institute of Technical Sciences, Hipolit Cegielski State University of Applied Sciences, Wrzesińska 43-55, 62-200 Gniezno, Poland

Abstract: The investigation and clarification of the properties of surface-functionalized superparamagnetic nanoparticles in a biological environment are key challenges prior to their medical applications. In the present work, electron paramagnetic resonance spectroscopy (EPR) combined with the spin labeling technique was utilized to better understand the behavior of nitroxides attached to magnetite nanoparticles dispersed in body fluid. EPR spectra of spin-labeled, silane-coated Fe₃O₄ nanoparticles in human serum and whole blood were recorded and analyzed for both room- and low-temperature values. In all cases, the obtained EPR signal consisted of a broad line from magnetite cores and a characteristic signal from the attached 4-Amino-2,2,6,6-tetramethylpiperidine-1-oxyl (4-amino-TEMPO). Even for liquid samples, the anisotropic components of magnetic tensors did not fully average out, which was reflected in the differences in the intensity of three narrow hyperfine lines from nitroxide. At 230 K the irregular slow-motion signal from the attached radical was also simulated using the EasySpin toolbox, which allowed to determine the parameters related to magnetic tensors and the dynamics of the spin label. The study showed that the anisotropy of the motion of the spin label 4-amino-TEMPO reflects its interactions with the surrounding medium and the manner of the attachment of the nitroxide to the surface of nanoparticles.

Keywords: magnetic nanoparticles; iron oxide; spin labels; TEMPO; EPR spectroscopy; blood; serum



Citation: Kubiak, T. The Influence of Blood and Serum Microenvironment on Spin-Labeled Magnetic Nanoparticles. *Magnetism* **2024**, *4*, 114–124. <https://doi.org/10.3390/magnetism4020009>

Academic Editor: Paola Tiberto

Received: 20 February 2024

Revised: 4 April 2024

Accepted: 2 May 2024

Published: 10 May 2024



Copyright: © 2024 by the author. Licensee MDPI, Basel, Switzerland. This article is an open access article distributed under the terms and conditions of the Creative Commons Attribution (CC BY) license (<https://creativecommons.org/licenses/by/4.0/>).

1. Introduction

Scientists' interest in studying superparamagnetic iron oxide nanoparticles has not waned for many years. The reason is the large number of potential biomedical applications that these particles may have in diagnostics and therapy. One can mention contrast enhancement in magnetic resonance imaging [1], magnetic hyperthermia treatment [2], detoxification of biological fluids [3], magnetic separation of cancer cells [4] or alternating magnetic field-induced thermal strengthening of the shells of microcapsules and liquid marbles [5].

Magnetite nanoparticles have many favorable properties. However, in order to ensure their stability and biocompatibility, it is necessary to cover them with an appropriate polymer. One should remember that broadly defined biocompatibility is understood not only as a lack of toxicity and immunogenicity, but also the ability to perform the planned role in the biological environment [6]. Therefore, it is important to investigate the behavior of functionalized nanoparticles in various media, especially in aqueous solutions and body fluids such as plasma or blood. It is often assumed that nanoparticles could reach their destination through the bloodstream [7,8].

Electron paramagnetic resonance (EPR) spectroscopy is a recognized technique for testing samples containing unpaired electrons. When such a specimen is placed in an external magnetic field, the energy levels are split, which is known as the Zeeman effect. The energy of individual levels depends on the orientation of the spin and the associated magnetic moment. When the system is supplied with a quanta of electromagnetic radiation

of microwave frequency ν and the quantum energy value $h\nu$ is equal to the energy difference ΔE between the split energy levels, the resonance condition is fulfilled:

$$\Delta E = h\nu = g\mu_B B_r$$

where g is the spectroscopic splitting factor that allows one to distinguish a specific paramagnetic center, μ_B is the Bohr magneton, B_r is resonance magnetic field induction, and h is Planck's constant.

EPR spectroscopy may be useful for studying the properties of magnetic nanoparticles, especially when determining their actual composition. For example, it is possible to identify the specific type of iron oxide present in a sample and find out the degree of maghemitization (oxidation) of a magnetite material [9]. The typical EPR spectrum of Fe_3O_4 nanoparticles is dominated by a distinct signal coming from their magnetic core. This signal differs between samples depending on the properties of the surface as well as the interaction with the environment. Therefore, the features of the EPR spectra of the magnetic core were different for iron(II,III) oxide nanoparticles functionalized with silane and dextran [10], PEG-coated magnetite nanoparticles in whole human blood [11], chitosan covered magnetite nanoparticles in water and standardized (sodium alginate and calcium chloride) hydrogel [12], or magnetosomes (nanoparticles isolated from the magnetotactic bacteria) dispersed in water or HEPES buffer [13].

Attaching a spin label (organic molecule with an unpaired electron) to nanoparticles expands the possibilities of using EPR spectroscopy for studies of molecular dynamics in liquids or ordered phases, such as biological membranes. EPR measurements can not only provide the useful information about the microenvironment of this label, and the polarity and viscosity of its surroundings, but also supply us with valuable details about processes occurring at the interface in the case of molecules immobilized on the surface of a solid material [14]. Spin labels are often based on nitroxide moiety, which constitutes a stable paramagnetic center with an unpaired electron delocalized over the N-O• group [15]. Among the nitroxides used as spin labels and probes, the TEMPO (2,2,6,6-Tetramethylpiperidin-1-yl)oxyl derivatives are the most popular. The magnetic interaction between the unpaired electron and the spin of the ^{14}N nitrogen nucleus ($I = 1$) in the nitroxide results in hyperfine splitting, and thus the recorded EPR spectrum takes the form of three lines. In the solution, the value of the isotropic hyperfine coupling constant A depends on the structure of the radical and the properties of the medium, and is determined by the distance between neighboring components of the EPR spectrum [16]. Although the spin labeling technique is primarily associated with investigations of proteins and biological membranes, it has also been used in the study of nanoparticles. One can mention the research concerning TEMPOL sensors and magnetite nanoparticles in aqueous solutions and dried gelatin films [16], nitroxide-doped magnetic fluids [17], 4-Amino-TEMPO-labeled Fe_3O_4 [18] and gold nanoparticles [19]. Interesting applications include the tracking of the diffusion of TEMPO-labeled, polymer-coated magnetite nanoparticles within the hydrogel medium using the L-band (1 GHz) electron paramagnetic resonance imaging (EPRI) technique [12] and X-band (9.4 GHz) monitoring of the interactions between TEMPO-functionalized magnetic nanoparticles and yeast cells [20].

The subject of interest of the present article is the application of EPR spectroscopy to investigate the behavior of the 4-amino-TEMPO spin label attached to silane-coated magnetite nanoparticles dispersed in human serum and whole blood, and in particular to determine the influence of this biological microenvironment on the dynamics of the rotational movement of nitroxide radicals present on the surfaces of the nanoparticles.

2. Materials and Methods

2.1. Experimental Section

The samples were prepared based on commercially available Fe_3O_4 nanoparticles purchased from Sigma-Aldrich (Saint Louis, MI, USA). According to the product specification, their average core diameter was 5 ± 1 nm (from TEM measurements) and the magnetization

was ≥ 30 emu/g (under 4500 Oe and at ambient temperature). Nanoparticles were coated with silane and functionalized at the Faculty of Chemistry Adam Mickiewicz University in Poznań, Poland using the method presented in [21]. The role of the silane was to create a protective shell and introduce functional groups that enabled the covalent attachment of the 4-amino-TEMPO spin label. The schematic representation of H₂N-TEMPO is depicted in Figure 1a. The tested nanoparticle samples 1 and 2 differed slightly in the method of attaching the nitroxide to the nanoparticle core, as shown in Figure 1b.

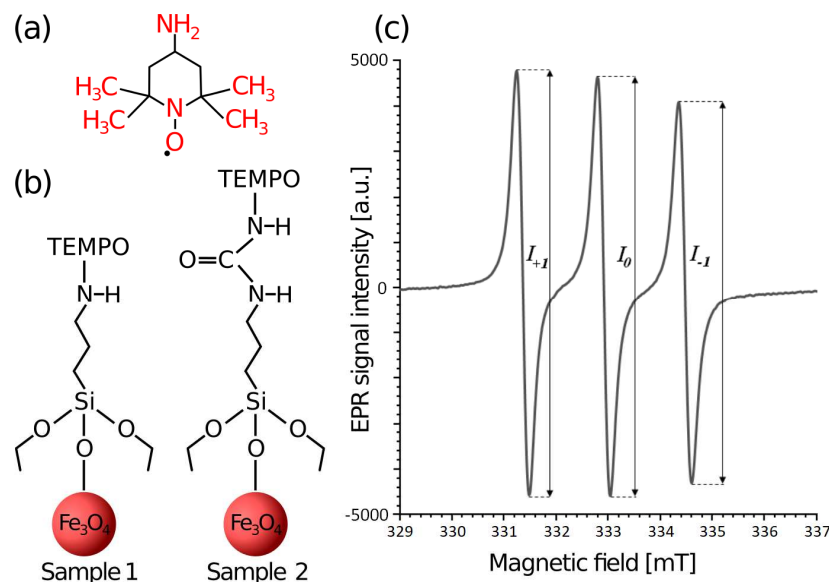


Figure 1. (a) Structure of H₂N-TEMPO. (b) The method of attaching the nitroxide radical to magnetite nanoparticles using silanes with various functional groups for samples 1 and 2. (c) The method of determining the heights of individual lines in the case of the spin label in the fast rotation regime.

Samples of human serum and whole blood (containing both morphological elements and plasma) were obtained from the Greater Poland Cancer Center in Poznań. The potassium EDTA anticoagulant was used to prevent the blood from clotting and enable storage.

Samples for EPR measurements were prepared by mixing 30 μ L of the nanoparticle colloidal suspension (0.1 mg/mL) with 30 μ L of serum or whole human blood for 20 min. Then, 55 μ L of the prepared mixture was taken into a vial or disposable capillary in the case of measurements at room temperature.

EPR measurements were performed using a Bruker EMX-10 (Bruker Instruments, Billerica, MA, USA) continuous wave spectrometer, which operates in the X-band (9.4 GHz). The tested samples were placed in a standard rectangular resonator ER 4102ST (Bruker BioSpin, Billerica, MA, USA). Measurements at low temperature were made using the ER 4131VT digital temperature control system. The cooling medium was N₂ gas obtained by heating liquid nitrogen. The temperature in the vicinity of the sample was controlled using a thermocouple and automatically stabilized with an accuracy of 0.1 K. For frozen samples, the signal from the spin label H₂N-TEMPO attached to nanoparticles was recorded using the following spectrometer settings: sweep range 20 mT centered at 335 mT, modulation amplitude 0.1 mT (modulation frequency 100 kHz), and time constant of 40.96 ms. Spin-labeled nanoparticles in serum and whole human blood were also tested in liquid form in capillaries at room temperature 293 K. In this case, a modulation amplitude of 0.05 mT was used. Additionally, in all cases, the whole EPR spectrum of magnetite nanoparticles was recorded in a wide sweep range of 650 mT. The stability of the measurement conditions was checked using a standard sample in the form of a ruby crystal ($g \approx 4.3$).

2.2. Analysis of Spectra and Simulations

The method of analyzing the spectra of the H₂N-TEMPO attached to the nanoparticles depended on the rotational mobility of this label, which was reflected in the width and the shape of the signal. In general, fast rotation occurs when the spin label is in a medium with low density and viscosity (e.g., water) and the sample is in a liquid state. For a spin label in the fast rotation regime, the rotational correlation time τ_R was calculated using the formula:

$$\tau_R = 6.51 \cdot 10^{-10} \Delta B_0 \left(\sqrt{\frac{I_0}{I_{+1}}} + \sqrt{\frac{I_0}{I_{-1}}} - 2 \right) \quad (1)$$

where ΔB_0 is the peak-to-peak width of the central line (in Gauss unit: 1 Gs = 10⁻⁴ T) and I_0 , I_{+1} , I_{-1} are the heights of the central, low-field and high-field lines, respectively [12,19]. The method of determining the above-mentioned line heights for the spectrum of a spin label H₂N-TEMPO attached to nanoparticles in the fast rotation regime is shown in Figure 1c. The hyperfine coupling constant was determined as the spacing between neighboring peaks. Information about the anisotropy of the spin label motion was obtained by analyzing the relative intensities of the hyperfine components, and expressed by the dimensionless parameter ε :

$$\varepsilon = \frac{\sqrt{\frac{I_0}{I_{+1}}} - 1}{\sqrt{\frac{I_0}{I_{-1}}} - 1} \quad (2)$$

At low temperatures (and also in the more viscous media), the spin label remains in the slow-motion regime. In such a situation, the analysis of EPR spectra was more difficult due to the fact that the partial averaging of the spectrum by molecular motion and spin dynamics resulted in more complex and irregular line shapes. Therefore, in order to interpret them properly, taking into account both parameters related to magnetic tensors and the dynamics, computer simulations had to be performed.

Simulations of the EPR spectra of the 4-amino-TEMPO spin label attached to the nanoparticles were performed using EasySpin—the open-source MATLAB toolbox. Depending on the time scale of the nitroxide rotation dynamics, different functions can be used in the simulations: “pepper” for the completely immobilized paramagnetic molecule (rigid limit), “chili” for the slowly rotating label (slow motion), and “garlic” for the rapid tumbling (fast-motion regime) [22]. In the present work, EPR signals of the 4-amino-TEMPO spin label attached to nanoparticles were simulated for temperature 230 K using the “chili” function. Additionally, thanks to the use of the “esfit” function and the Nelder/Mead downhill simplex method, the program was able to dynamically change the values of the simulation parameters until an optimal match between the simulated and experimental spectra was achieved. Simulations were performed on the basis of spectra recorded in the 20 mT sweep range. When the signal from the 4-amino-TEMPO in the experimental spectrum appeared on the slope of a broad line from the magnetite core of the nanoparticles, a contribution of this broad line was subtracted. Thanks to this, the nitroxide spectra had a well-corrected baseline. For the slowly rotating labels, performing the simulation allowed us to determine such parameters as line width, rotational correlation time τ_R , and the values of tensor components: \check{g} (g_x, g_y, g_z) and \check{A} (A_x, A_y, A_z).

3. Results

3.1. EPR Spectra at Room Temperature

Silane-coated and 4-amino-TEMPO-labeled magnetite nanoparticles (samples 1 and 2) were first tested in serum and whole blood at room temperature (≈ 293 K) in the measurement capillaries. The EPR spectrum of such nanoparticles consisted of a broad line from magnetite cores (peak-to-peak EPR linewidth $\Delta B_{pp} \approx 27$ mT) and a triplet from nitroxides, as shown in Figure 2a. Three characteristic hyperfine lines originating from the 4-amino-TEMPO attached to nanoparticles dispersed in the above-mentioned media were

also recorded in the narrower sweep range. These spectra are shown in Figure 2b–e for both samples.

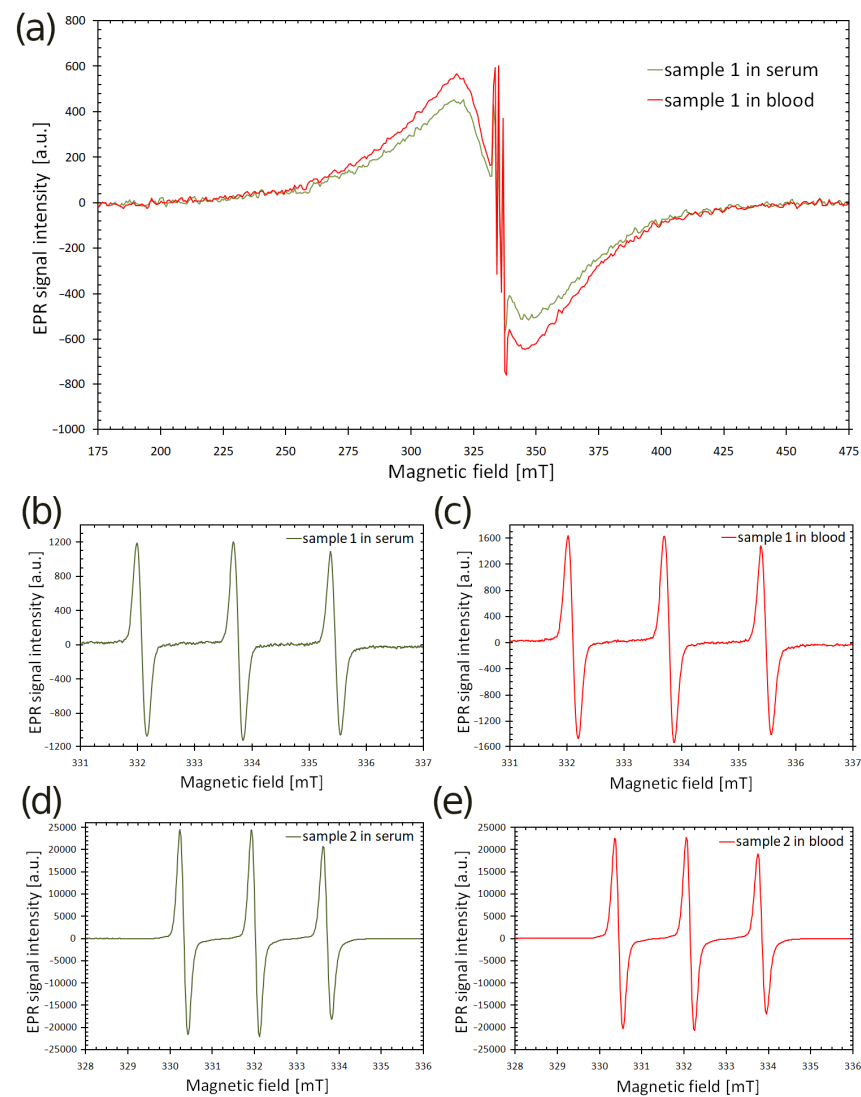


Figure 2. EPR spectra of spin-labeled Fe_3O_4 nanoparticles at room temperature. (a) Whole spectrum in a wide sweep range. Triplets from attached nitroxide radical in serum (b) and whole blood (c) for sample 1 and analogously for sample 2 (d,e).

Table 1 contains the parameters of the spectra of the spin label attached to nanoparticles in the tested media along with the measurement uncertainties. The values of rotational correlation time τ_R and anisotropy coefficient ε were calculated using Equations (1) and (2), respectively.

Table 1. Calculated values of g factor, hyperfine constant A_{izo} , rotational correlation time τ_R and anisotropy coefficient ε for the $\text{H}_2\text{N-TEMPO}$ attached to nanoparticles (samples 1 and 2) in human serum and whole blood at room temperature.

Sample	g	A_{izo} (mT)	τ_R (s)	ε
sample 1 in serum	2.0058 (± 0.0002)	1.691 (± 0.014)	$5.2 \cdot 10^{-11}$ ($\pm 0.5 \cdot 10^{-11}$)	0.32 (± 0.03)
sample 1 in blood	2.0059 (± 0.0002)	1.681 (± 0.014)	$6.3 \cdot 10^{-11}$ ($\pm 0.6 \cdot 10^{-11}$)	0.18 (± 0.02)
sample 2 in serum	2.0059 (± 0.0002)	1.681 (± 0.014)	$1.13 \cdot 10^{-10}$ ($\pm 0.18 \cdot 10^{-10}$)	0.057 (± 0.007)
sample 2 in blood	2.0058 (± 0.0002)	1.701 (± 0.014)	$1.35 \cdot 10^{-10}$ ($\pm 0.20 \cdot 10^{-10}$)	0.068 (± 0.008)

3.2. EPR Spectra of Frozen Samples

The EPR spectra of both nanoparticle samples in serum and whole human blood were also recorded at 230 K in sweep ranges of 650 and 20 mT. Also, in this case, the full spectrum (Figure 3a) consisted of a broad line from the nanoparticle cores ($\Delta B_{pp} \approx 42$ mT), accompanied by a signal from the attached nitroxide. The shape of the EPR signal from the 4-amino-TEMPO in both tested media at 230 K (see Figure 3b–e) indicates that the movement of the label was significantly hindered.

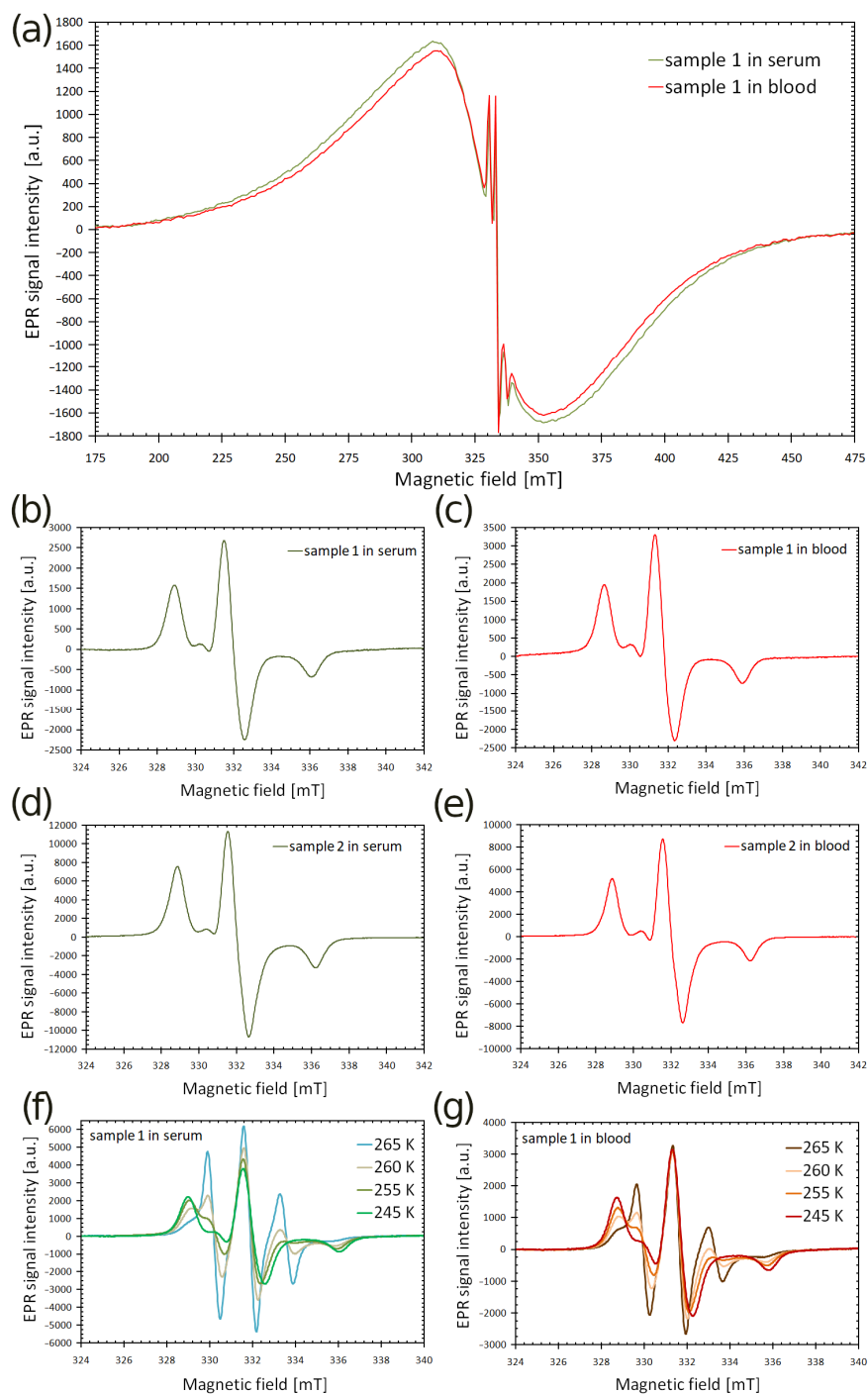


Figure 3. EPR spectra of spin-labeled Fe_3O_4 nanoparticles at 230 K. (a) Whole spectrum in a wide sweep range. Signals from attached nitroxide radical in serum (b) and whole blood (c) for sample 1 and analogously for sample 2 (d,e). The changes in the shape of the EPR signal from the attached spin label in serum (f) and whole blood (g) upon heating in the temperature range of 245–265 K.

For sample 1, EPR spectra were additionally recorded in the temperature range of 245–265 K to show how the dynamics of the nitroxide movement change when the sample is heated (look at Figure 3f–g). The spectra of the nitroxide radical attached to nanoparticles were simulated for a temperature of 230 K using the EasySpin software. The results for both media and nanoparticle samples are presented in Figure 4. The figures include also the parameters of the EPR spectra obtained as a result of the simulations: the values of the rotational correlation time τ_R , the line width, the components of the \hat{g} tensor (g_x , g_y and g_z) and the hyperfine tensor \hat{A} (A_x , A_y and A_z).

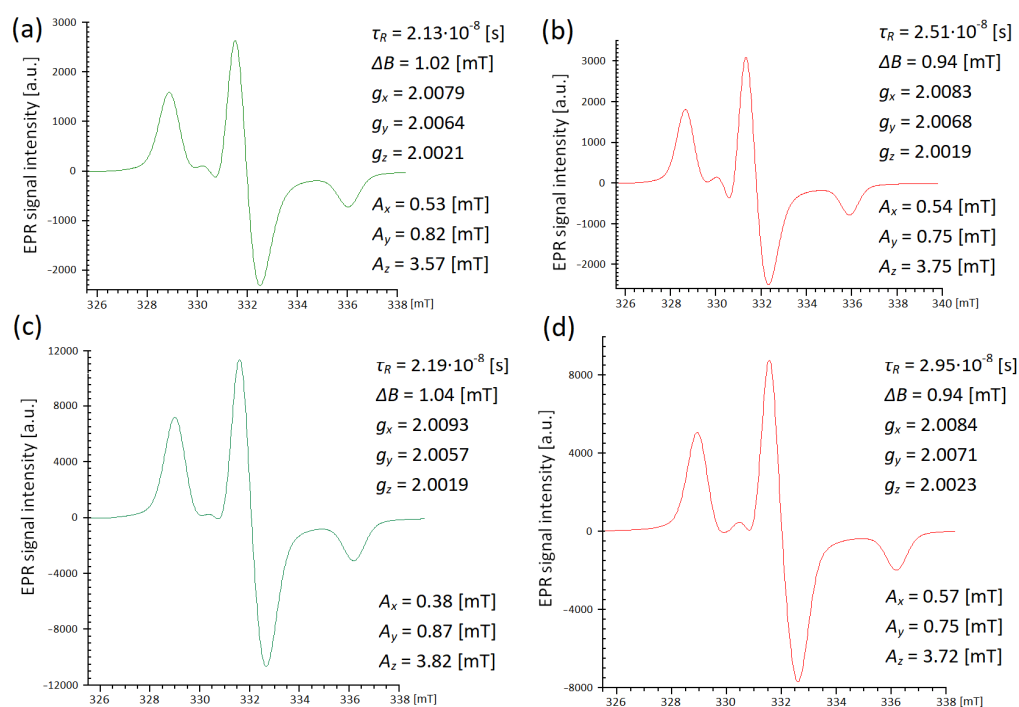


Figure 4. The simulated spectra of the nitroxide radical attached to nanoparticles for sample 1 in serum (a) and whole blood (b) and for sample 2 in serum (c) and whole blood (d). The obtained values of rotational correlation time τ_R , line width, and components of the \hat{g} tensor and the hyperfine tensor \hat{A} are included.

4. Discussion

The broad EPR line, recorded for all samples in a wide sweep range, comes from magnetite cores and is characteristic of nanoparticles that constitute single magnetic domains. The particles used in the experiments had an average core size of 5 nm. It is worth recalling that according to the literature, iron oxide nanoparticles with a diameter below ≈ 30 nm act as single-domain magnets with superparamagnetic properties [23]. The EPR lines from the core of the nanoparticles were narrower at room temperature 293 K than at 230 K. Such broadening of the EPR lines during sample cooling is characteristic of iron oxide nanoparticles, and was previously observed for magnetite nanoparticles stabilized with chitosan [12] and poly(ethylene glycol) [11]. If nanoparticles are randomly oriented in a macroscopically isotropic sample, the angular dependence of their resonance fields results in the broadening of the spectrum [24]. Such a random distribution of the anisotropy axes with respect to the magnetic field becomes more pronounced at low temperatures, when the signal widening effect is particularly visible [25]. A broad EPR signal from the core can be treated as a superposition of multiple lines that differ in their resonance field due to the presence of magnetocrystalline anisotropy [26]. In general, depending on the size of the magnetic particles, four types of anisotropy might be responsible for the occurrence of internal fields; these include magnetocrystalline anisotropy, shape anisotropy, anisotropy of domain structures and exchange anisotropy [9]. Internal fields originating from the above-mentioned

contributions add to the external field of the spectrometer, creating an effective field. The size dispersion of nanoparticles in the sample can influence the magnetic properties of the whole specimen. The topic of the influence of temperature and core dimensions on the magnetic properties of nanoparticles has been recently discussed in several articles, in the context of both theoretical simulations [27] and experimental research [28,29].

Since the behavior of the main line originating from the cores is relatively well known, it is worth focusing on the analysis of the signal from the nitroxide radical attached to the nanoparticles dispersed in serum and whole human blood.

In the case of a spin label 4-amino-TEMPO, an electron with spin $S = \frac{1}{2}$ interacts with the ^{14}N nitrogen nucleus with spin $I = 1$. As a result, we observed three lines of hyperfine structure. For liquid samples, the intensities of the individual triplet lines differed, which means that the anisotropic components of the \hat{g} and \hat{A} tensors did not fully average out. Although the line intensity ratios varied depending on the sample and medium, the general tendency was that the high-field component had the lowest amplitude. It is known from the literature that the EPR spectra of nitroxides attached to nanoparticles often have a distorted line at high field due to a hindered rotation and the accompanying increase in τ_R [19]. The low field line and the center line were quite similar, but the latter had a slightly larger amplitude in all cases. Therefore, the value of anisotropy parameter ε was >0 . Since in the current research the ε coefficient did not take negative values, we cannot assume that the nitroxide rotated most rapidly along the axis perpendicular to the surface of the nanoparticles, as was the case of TEMPO-labeled, chitosan-coated nanoparticles in toluene, which were studied in the past [12]. Additionally, the ε values for nitroxide from sample 2 were lower than those from sample 1. This confirms that the dynamics of the spin label movement for these samples was different due to the distinct way of attaching nitroxide to the silane on the surface of the nanoparticles. As mentioned earlier, for liquid samples at room temperature, rotational correlation times were estimated based on the measurements of the intensity of individual peaks, using Equation (1). In general, it can be summarized that for a given sample, the value of τ_R in serum is smaller than the value of τ_R in blood. The factor that most significantly influenced the observed values of correlation times was the viscosity of the medium, because in the more viscous microenvironment, the spin-label rotated slower. The viscosity of whole blood (3.5–5.5 cP) exceeds the viscosity of plasma (1.2–1.3 cP), but it should be borne in mind that it is influenced by many factors, e.g., hematocrit and the rheological properties of red blood cells [30]. The viscosity of serum due to the lack of fibrinogen is even lower than the viscosity of plasma. The present EPR measurements confirm that the microviscosity of the surroundings of nanoparticles in blood is greater than that of serum.

In the case of frozen samples 1 and 2 in both media, the irregular shapes of the signals from 4-amino-TEMPO attached to nanoparticles indicate that the movement of nitroxide was strongly hindered. The spectra recorded at 230 K and presented in Figure 3b–e are characteristic of the so-called slow-motion regime. These spectra were also simulated using the EasySpin program (Figure 4), taking into account parameters related to magnetic tensors as well as those related to dynamics. At 230 K, the rotational correlation time values determined on the basis of the simulations are in the order of 10^{-8} s. It is worth recalling that for the liquid samples in the fast rotation regime (room temperature), the τ_R values were much shorter, in the order of 10^{-10} – 10^{-11} s. It is therefore certain that as the sample is cooled down, the nitroxide motion significantly slows down too. The simulations of spectra recorded at low temperatures also confirm that τ_R (in blood) $>$ τ_R (in serum). This is evidence that the properties of the medium also influence the dynamics of the spin label attached to nanoparticles at low temperatures, when the molecular motion is partially hindered. Differences between samples 1 and 2 may indicate the effect of the mode of attaching the label to magnetite nanoparticles on its rotation in a given medium. The line width value ΔB , obtained as a result of the simulation, also varied depending on the environment. At 230 K, ΔB had a lower value for 4-amino-TEMPO attached to nanoparticles in whole blood, and there was a slightly higher value when the medium was serum. The

spectrum of the TEMPO radical at low temperature may broaden, which is caused by dipolar interactions between the nitroxide molecules. Such behavior is most noticeable for free TEMPO in the pure water [31]. In the case of the H₂N-TEMPO attached to nanoparticles in blood and serum, a shielding effect of nitroxide microenvironment components can be assumed. In whole blood, in addition to serum proteins, there are also morphotic elements, which, on the one hand, may slow down the motion of the nitroxide, but on the other hand, reduce the widening of the line due to the additional weakening of the interactions between the label molecules. It is also worth commenting on the spectra presented in Figure 3f–g. Heating the sample from 230 to 265 K allowed us to show how the EPR signal from nitroxides attached to nanoparticles changed depending on the temperature. As the temperature rose, the rotation dynamics of the nitroxide radical gradually increased. This was reflected in the shape of the EPR spectrum, which steadily narrowed and turned into a distinct triplet. Also in this case, it turned out that the movement of the spin label at a given temperature was influenced by the properties of the microenvironment.

5. Conclusions

Functionalized superparamagnetic iron oxide nanoparticles with an attached 4-amino-TEMPO spin label were characterized by a two-fold EPR spectrum: a broad line from magnetite cores and a characteristic signal from nitroxides. Even for liquid samples, three narrow lines of hyperfine structure differed slightly in the intensity, which means that the anisotropic components of the \hat{g} and \hat{A} tensors did not fully average out. In the case of frozen specimens, the irregular shape of the signal indicates that the movement of nitroxide was strongly hindered. Therefore, determining the parameters related to magnetic tensors and dynamics required performing computer simulations.

The dynamics of the spin label varied depending on the environment in which the nanoparticles were dispersed. The rotational correlation times for the nitroxide radicals attached to nanoparticles in the whole human blood had higher values compared to nanoparticles in serum. The factors that significantly influenced the experimentally determined values of τ_R were: temperature and the viscosity of the medium. The mode of bonding the nitroxide radical to the surface of nanoparticles (using silanes with various functional groups) was also reflected in the anisotropy of its movement, and affected the interaction of nanoparticles with the environment.

Funding: This research received no external funding.

Institutional Review Board Statement: Not applicable.

Informed Consent Statement: Not applicable. EPR studies did not require direct human participation. Biological material was provided by an external institution and was not linked to any personal data.

Data Availability Statement: Data are contained within the article.

Acknowledgments: The author would like to thank Joanna Kurczewska (Faculty of Chemistry AMU Poznań) for providing magnetite nanoparticles, and the staff of the Greater Poland Cancer Center in Poznań for providing samples of whole blood and human serum. Bernadeta Dobosz is thanked for co-supervision during research performed at AMU. The author would like to express special gratitude to Ryszard Krzyminiewski, who passed away in May 2022, for several years of scientific supervision and valuable advice.

Conflicts of Interest: The author declares no conflicts of interest.

References

1. Oberdick, S.D.; Jordanova, K.V.; Lundstrom, J.T.; Parigi, G.; Poorman, M.E.; Zabow, G.; Keenan, K.E. Iron oxide nanoparticles as positive T₁ contrast agents for low-field magnetic resonance imaging at 64 mT. *Sci. Rep.* **2023**, *13*, 11520. [[CrossRef](#)]
2. Palzer, J.; Eckstein, L.; Slabu, I.; Reisen, O.; Neumann, U.P.; Roeth, A.A. Iron Oxide Nanoparticle-Based Hyperthermia as a Treatment Option in Various Gastrointestinal Malignancies. *Nanomaterials* **2021**, *11*, 3013. [[CrossRef](#)]
3. Gupta, A.K.; Gupta, M. Synthesis and surface engineering of iron oxide nanoparticles for biomedical applications. *Biomaterials* **2005**, *26*, 3995–4021. [[CrossRef](#)] [[PubMed](#)]

4. Xu, H.; Aguilar, Z.P.; Yang, L.; Kuang, M.; Duan, H.; Xiong, Y.; Wei, H.; Wang, A. Antibody conjugated magnetic iron oxide nanoparticles for cancer cell separation in fresh whole blood. *Biomaterials* **2011**, *32*, 9758–9765. [[CrossRef](#)]
5. Bielas, R.; Kubiak, T.; Kopčanský, P.; Šafařík, I.; Józefczak, A. Tunable particle shells of thermo-responsive liquid marbles under alternating magnetic field. *J. Mol. Liq.* **2023**, *391*, 123283. [[CrossRef](#)]
6. Kubiak, T. Polymeric capsules and micelles as promising carriers of anticancer drugs. *Polim. Med.* **2022**, *52*, 37–50. [[CrossRef](#)] [[PubMed](#)]
7. Mykhaylyk, O.; Dudchenko, N.; Dudchenko, A. Doxorubicin magnetic conjugate targeting upon intravenous injection into mice: High gradient magnetic field inhibits the clearance of nanoparticles from the blood. *J. Magn. Magn. Mater.* **2005**, *293*, 473–482. [[CrossRef](#)]
8. Predoi, S.-A.; Iconaru, S.L.; Predoi, D. In Vitro and In Vivo Biological Assays of Dextran Coated Iron Oxide Aqueous Magnetic Fluids. *Pharmaceutics* **2023**, *15*, 177. [[CrossRef](#)] [[PubMed](#)]
9. Fischer, H.; Luster, J.; Gehring, A.U. EPR evidence for maghemitization of magnetite in a tropical soil. *Geophys. J. Int.* **2007**, *169*, 909–916. [[CrossRef](#)]
10. Dobosz, B.; Krzyminiwski, R.; Kurczewska, J.; Schroeder, G. The influence of surface modification, coating agents and pH value of aqueous solutions on physical properties of magnetite nanoparticles investigated by ESR method. *J. Magn. Magn. Mater.* **2017**, *429*, 203–210. [[CrossRef](#)]
11. Kubiak, T.; Krzyminiwski, R.; Dobosz, B.; Schroeder, G.; Kurczewska, J.; Hałupka-Bryl, M. A study of magnetite nanoparticles in whole human blood by means of electron paramagnetic resonance. *Acta Bio-Opt. Inf. Med. Biomed. Eng.* **2015**, *21*, 9–15.
12. Krzyminiwski, R.; Kubiak, T.; Dobosz, B.; Schroeder, G.; Kurczewska, J. EPR spectroscopy and imaging of TEMPO-labeled magnetite nanoparticles. *Curr. Appl. Phys.* **2014**, *14*, 798–804. [[CrossRef](#)]
13. Bielas, R.; Kubiak, T.; Molcan, M.; Dobosz, B.; Rajnak, M.; Józefczak, A. Biocompatible Hydrogel-Based Liquid Marbles with Magnetosomes. *Materials* **2024**, *17*, 99. [[CrossRef](#)] [[PubMed](#)]
14. Tudose, M.; Constantinescu, T.; Balaban, A.T.; Ionita, P. Synthesis and electron paramagnetic resonance study of a nitroxide free radical covalently bonded on aminopropyl-silica gel. *Appl. Surf. Sci.* **2008**, *254*, 1904–1908. [[CrossRef](#)]
15. Torricella, F.; Pierro, A.; Mileo, E.; Belle, V.; Bonucci, A. Nitroxide spin labels and EPR spectroscopy: A powerful association for protein dynamics studies. *Biochim. Biophys. Acta Proteins Proteom.* **2021**, *1869*, 140653. [[CrossRef](#)] [[PubMed](#)]
16. Kovarski, A.L.; Sorokina, O.N. Study of local magnetic fields and magnetic ordering in fluid and solid matrices containing magnetite nanoparticles using TEMPOL stable radical. *J. Magn. Magn. Mater.* **2007**, *311*, 155–161. [[CrossRef](#)]
17. Morais, P.C.; Alonso, A.; Silva, O.; Buske, N. Electron paramagnetic resonance of nitroxide-doped magnetic fluids. *J. Magn. Magn. Mater.* **2002**, *252*, 53–55. [[CrossRef](#)]
18. Zhao, H.; Zhang, Z.; Zhao, Z.; Yu, R.; Wan, Y.; Lan, M. Preparation and characterization of novel spin labeled magnetic nanoparticles. *Adv. Mat. Lett.* **2011**, *2*, 172–175. [[CrossRef](#)]
19. Chechik, V.; Wellsted, H.J.; Korte, A.; Gilbert, B.C.; Caldararu, H.; Ionita, P.; Caragheorghopol, A. Spin-labelled Au nanoparticles. *Farad. Disc.* **2004**, *125*, 279–291.
20. Krzyminiwski, R.; Dobosz, B.; Schroeder, G.; Kurczewska, J. ESR as a monitoring method of the interactions between TEMPO-functionalized magnetic nanoparticles and yeast cells. *Sci. Rep.* **2019**, *9*, 18733.
21. Wu, W.; He, Q.; Jiang, C. Magnetic Iron Oxide Nanoparticles: Synthesis and Surface Functionalization Strategies. *Nanoscale Res. Lett.* **2008**, *3*, 397–415. [[CrossRef](#)] [[PubMed](#)]
22. Stoll, S.; Schweiger, A. Easy spin: Simulating cw ESR spectra. In *ESR Spectroscopy in Membrane Biophysics*; Hemminga, M.A., Berliner, L.J., Eds.; Springer: New York, NY, USA, 2007; Volume 27, pp. 299–321.
23. Pucci, C.; Degl'Innocenti, A.; BelenliGümüş, M.; Ciofani, G. Superparamagnetic iron oxide nanoparticles for magnetic hyperthermia: Recent advancements, molecular effects, and future directions in the omics era. *Biomater. Sci.* **2022**, *10*, 2103–2121. [[CrossRef](#)] [[PubMed](#)]
24. Kliava, J.; Berger, R. Size and shape distribution of magnetic nanoparticles in disordered systems: Computer simulations of superparamagnetic resonance spectra. *J. Magn. Magn. Mater.* **1999**, *205*, 328–342. [[CrossRef](#)]
25. Vázquez-Victorio, G.; Acevedo-Salas, U.; Valenzuela, R. Microwave Absorption in Nanostructured Spinel Ferrites. In *Ferromagnetic Resonance—Theory and Applications*; Yalcina, O., Ed.; InTech: Rijeka, Croatia, 2013; pp. 169–194.
26. Flores-Arias, Y.; Vazquez-Victorio, G.; Ortega-Zempoalteca, R.; Acevedo-Salas, U.; Ammar, S.; Valenzuela, R. Magnetic phase transitions in ferrite nanoparticles characterized by electron spin resonance. *J. Appl. Phys.* **2015**, *117*, 17A503.
27. Tran, H.B.; Matsushita, Y. Temperature and size dependence of energy barrier for magnetic flips in L1₀FePt nanoparticles: A theoretical study. *Scr. Mater.* **2024**, *242*, 115947.
28. García-Acevedo, P.; González-Gómez, M.A.; Arnosa-Prieto, Á.; de Castro-Alves, L.; Piñeiro, Y.; Rivas, J. Role of Dipolar Interactions on the Determination of the Effective Magnetic Anisotropy in Iron Oxide Nanoparticles. *Adv. Sci.* **2023**, *10*, 2203397. [[CrossRef](#)] [[PubMed](#)]
29. Sadat, M.E.; Bud'ko, S.L.; Ewing, R.C.; Xu, H.; Pauletti, G.M.; Mast, D.B.; Shi, D. Effect of Dipole Interactions on Blocking Temperature and Relaxation Dynamics of Superparamagnetic Iron-Oxide (Fe₃O₄) Nanoparticle Systems. *Materials* **2023**, *16*, 496. [[CrossRef](#)] [[PubMed](#)]

30. Nader, E.; Skinner, S.; Romana, M.; Fort, R.; Lemonne, N.; Guillot, N.; Gauthier, A.; Antoine-Jonville, S.; Renoux, C.; Hardy-Dessources, M.D.; et al. Blood Rheology: Key Parameters, Impact on Blood Flow, Role in Sickle Cell Disease and Effects of Exercise. *Front. Physiol.* **2019**, *10*, 1329. [[CrossRef](#)]
31. Santangelo, M.G.; Levantino, M.; Cupane, A.; Jeschke, G. Solvation of a Probe molecule by fluid supercooled water in a hydrogel at 200 K. *J. Phys. Chem. B* **2008**, *112*, 15546–15553. [[CrossRef](#)]

Disclaimer/Publisher's Note: The statements, opinions and data contained in all publications are solely those of the individual author(s) and contributor(s) and not of MDPI and/or the editor(s). MDPI and/or the editor(s) disclaim responsibility for any injury to people or property resulting from any ideas, methods, instructions or products referred to in the content.